 doi:10.20944/preprints201801.0213.v1

Article

Identification of Bichalcones as Sirtuin Inhibitors by Virtual Screening and *in Vitro* Testing

Berin Karaman [1,2,†], Zayan Alhalabi [2,†], Sören Swyter [3], Shetonde O. Mihigo [4], Kerstin Andrae-Marobela [5], Manfred Jung [3], Wolfgang Sippl [1] and Fidele Ntie-Kang [1.6,*]

[1] Department of Pharmaceutical Chemistry, Martin-Luther University of Halle-Wittenberg, Wolfgang-Langenbeck-Str. 4, 06120 Halle (Saale), Germany; karaman.berin@gmail.com (BK), zayan82at@hotmail.com (ZA), wolfgang.sippl@pharmazie.uni-halle.de (WS) and ntiekfidele@gmail.com (FNK)

[2] Department of Pharmaceutical Chemistry, Faculty of Pharmacy, Biruni University, Istanbul, Turkey; karaman.berin@gmail.com (BK)

[3] Institute of Pharmaceutical Sciences, Albert-Ludwigs-University of Freiburg, Albertstr. 25, 79104 Freiburg im Breisgau, Germany; soeren.swyter@pharmazie.uni-freiburg.de (SS) and manfred.jung@pharmazie.uni-freiburg.de (MJ)

[4] Department of Chemistry, University of Kinshasa, Kinshasa, DR Congo; smihigo@yahoo.com (SOM)

[5] Department of Biological Sciences, Faculty of Science, University of Botswana, Block 235, Private Bag, 0022 Gaborone, Botswana; k_marobela@yahoo.com (KAM)

[6] Department of Chemistry, University of Buea, P. O. Box 63, Buea, Cameroon; ntiekfidele@gmail.com (FNK)

* Correspondence: ntiekfidele@gmail.com (FNK); Tel.: +237-685-625-811

† These authors contributed equally and could be best regarded as joint first authors.

Abstract: Sirtuins are nicotinamide adenine dinucleotide (NAD^+)-dependent class III histone deacetylases and have been linked to the pathogenesis of numerous diseases such as HIV, metabolic disorders, neurodegeneration and cancer. Docking of the virtual pan-African natural products library (p-ANAPL), followed by *in vitro* testing, resulted in the identification of two inhibitors of sirtuin 1, 2 and 3 (sirt1-3). Two bichalcones; rhuschalcone IV (**8**) and rhuschalcone I (**9**), previously isolated from the medicinal plant *Rhus pyroides*, were shown to be active in the *in vitro* assay, with rhuschalcone I showing the best activity against sirt1, having an IC_{50} = 40.8 μM. Based on the docking experiments, suggestions for improving the biological activities of the newly identified hit compounds have been provided.

Keywords: bichalcones; sirtuin inhibitors; virtual screening.

1. Introduction

In the last few decades, natural products (NPs) or natural product derivatives have spurred great interest as re-fashionable sources for developing therapeutic agents against human diseases [1,2]. However, the isolation of NPs, the synthesis of their analogues and manufacturing them in larger quantities are major challenges that pharmaceutical companies face today [1-3]. Moreover, evaluating the potential of natural product agents with the available high throughput screening (HTS) techniques remains problematic [1, 4]. Although, combinatorial chemistry is still used to generate large compound libraries for HTS campaigns, a detailed analysis of approved drugs from 1981 to 2014 showed that only two actual combinatorial chemistry-derived drugs were approved; sorafenib (approved by the FDA in 2005) and ataluren (approved by the EMEA in 2014) [5]. Moreover, it was observed that among all the new therapeutic agents approved during the first 15 years of the 21st Century, 34 ± 9 % of drugs based on small molecules were either natural products or natural product-derived compounds [5].

 doi:10.20944/preprints201801.0213.v1

It had been shown that natural products from African botanical sources possess a unique and broad chemical space, with biological and drug-like properties exploitable in the field of drug discovery [6-9]. Docking and pharmacophore-based virtual screening (VS) campaigns conducted, for example, against a few selected known anti-cancer drug targets revealed the presence of potential anticancer agents within the newly developed AfroCancer database [6, 7]. The efforts of the pan-African Natural Products Library (p-ANAPL) consortium were aimed at collecting physical samples of NPs at a central location, which could then be directly available for screening purposes [10]. Owing to the small quantities of the isolated samples, an efficient approach for the management of the p-ANAPL library has been to only test samples of *in silico* hits from virtual screening. A previous successful campaign, which combined pharmacophore-based virtual screening and *in vitro* testing, had led to the identification of boldine and ixoratannin as anti-HIV-1 compounds [11]. These findings have prompted the search for potential inhibitors of sirtuins by *in silico* screening of the p-ANAPL library.

Recently, virtual screening for the identification of sirtuin inhibitors and modulators has received great interest [12-20]. Sirtuins are nicotinamide adenine dinucleotide (NAD^+)-dependent class III histone deacetylases that have been linked to the pathogenesis of numerous diseases such as HIV, metabolic disorders, neurodegeneration (including Alzheimer's disease and Parkinson's disease) and cancer [21-28]. Since the p-ANAPL library consists of compounds with a broad range of already reported activities, e.g. antibacterial, antiviral, anticancer, anti-inflammatory and properties [10], this collection represents a good starting point to search for novel inhibitors or modulators of sirtuins. Sirtuins share a highly conserved catalytic core composed of two subdomains; a large NAD^+ binding domain (Rossmann fold) and a smaller domain generated by two insertions in the NAD^+ binding domain, together with a helical module and a zinc-binding module [29, 30].

Within the last two decades, several sirt1 and sirt2 crystal structures have been solved in both apo and holo forms [31-43]. Ternary structures of sirt1 and sirt2 in complex with cofactor analogues, peptide-based and structurally diverse inhibitors revealed a high conformational flexibility in the catalytic pocket, especially in the extended C-pocket region. Thus, the experimentally known structures provide a good coverage of the conformational space of the catalytic pockets of sirt1 and -2 for a target-based VS campaign.

In the present work, we tested several of the reported crystal structures of Sirt1 and Sirt2 for virtually screening the p-ANAPL compound collection. The consideration of different protein conformations should increase the chance to identify novel actives. Several X-ray structures of sirt1 exist in the PDB, notably co-crystallized with a small molecule activator and inhibitor [44], together with sirt2 in complex with a macrocyclic peptide [41], a thiomyristoyl-lysine peptide [39], the cofactor fragments ADP ribose and nicotinamide [40], the inhibitor SirReal2 [40], and the indole derivative EX-243 [38], were considered for screening.

2. Results

2.1. Docking results

Docking of the p-ANAPL virtual compound collection, followed by selecting 5% of the top-ranked poses (GoldScore) yielded 22 hits for the substrate pocket of sirt1 (PDB ID: 4ZZJ) [45].

Preprints (www.preprints.org) | NOT PEER-REVIEWED | Posted: 23 January 2018 doi:10.20944/preprints201801.0213.v1

From the respective 22 hits, 5 compounds which had sufficient quantities were further retained for testing (Fig. S1, Supplementary Material). In a similar fashion, 5% of the top-ranked compounds were selected from docking experiments carried out onto the peptide (PDB IDs: 4R8M and 4L3O), the C (PDB ID: 4RMH) and the extended C (PDB ID: 5D7P) pocket of sirt2. The combined hit lists of sirt1 and sirt2 gave 13 compounds after the removal of duplicates and compounds forming unfavorable conformations within the respective binding sites (Fig. S1, Supplementary Material). Among the 13 selected compounds, only 7 had sufficient amounts (> 1 mg) for the screening assays within the p-ANAPL collection. All 7 selected compounds (**1**, **2**, **8**-**10**, **12** and **13**, Fig. 1) were tested in the assays against sirt1, 2 and 3. The entire virtual screening process for sirt1 and sirt2 has been summarised in Fig. S2 (Supplementary Material).

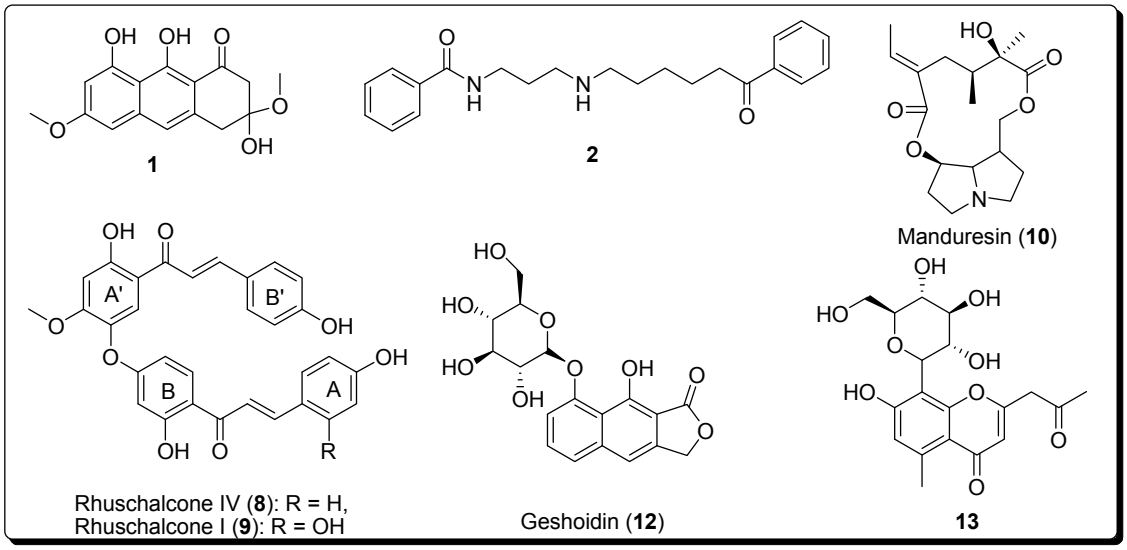

Figure 1. Compounds tested against Sirt1, -2 and -3.

2.2. In vitro activities

Among the selected compounds, compound **1**, **2**, **10**, **12** and **13** showed no inhibitory activity against sirt1, -2, and -3 at 50 μM concentration (Table 1). Meanwhile, compounds **8** and **9** showed moderate inhibitory effect against both sirt1 (**8**; IC_{50} = 46.7 ± 6.0, **9**; IC_{50} = 40.8 ± 8.5) and sirt2 (**8**; IC_{50} = 48.5 ± 39.5, **9**; IC_{50} = 44.8 ± 5.1). Nevertheless, sirt3 was only slightly affected at a 50μM concentration by compounds **8** and **9**.

Table 1. IC_{50} or percentage inhibitions @ 50 %of tested p-ANAPL compounds against sirt1, 2 and 3.

Compound number	Sirt 1	Sirt 2	Sirt 3
1 [b]	n.d. [c]	n.d. [c]	n.d. [c]
2	n.i. [a]	n.i. [a]	n.i. [a]
8	46.7 ± 6.0	48.5 ± 39.5	38 %
9	40.8 ± 8.5	44.8 ± 5.1	23 %
10	n.i. [a]	n.i. [a]	n.i. [a]
12 [b]	n.d.	n.d.	n.d.
13	n.i. [a]	n.i. [a]	n.i. [a]

[a] n.i. = no inhibition (< 10 %).

Preprints (www.preprints.org) | NOT PEER-REVIEWED | Posted: 23 January 2018 doi:10.20944/preprints201801.0213.v1

[b]autofluorescence.

[c] n.d. = not detectable. Note that activity not detectable due to the autofluorescence.

3. Discussion

The identified actives are rhuschalcones I and IV, respectively. These compounds have been previously isolated from the twigs [46] and root bark [47] of *Rhus pyroides* Burch (Anacardiaceae), a medicinal plant which is widely distributed in Eastern Botswana. This plant is also known to be the sources of several O-linked and C-C coupled bichalcones (Fig. 4) and biflavonoids, some of which have been obtained by total synthesis [48-52]. The rhuschalcones and their analogues are known to possess cytotoxic [47], antiprotozoal [48, 49] and carbonic anhydrase inhibitory [50] activities. Meanwhile, biflavones from this plant, e.g. agathisflavone and amentoflavone have shown an affinity for the $GABA_A$/benzodiazepine receptor [51].

It could be further proposed that analogues of the bichalcones (e.g. the O-linked littorachalcone or verbecharcone, verbenachalcone and rhuschalcones II and III, together with the C-C linked rhuschalcones V and VI, Fig. 2) be tested for sirt1, -2 and -3 inhibition. Also, the binding of these compounds in the extended C pocket could be tested in fluorescence assays. It could be suggested that, unlike the rhuschalcones, both C-C and C-O linked non-symmetrical bichalcones be also be synthesized tested against the sirtuins, with the view of investigating potential selectivities against the isoforms. Besides, chalcones have previously shown deacetylase inhibitory properties against sirt1 and cell growth in HEK293T cells [53].

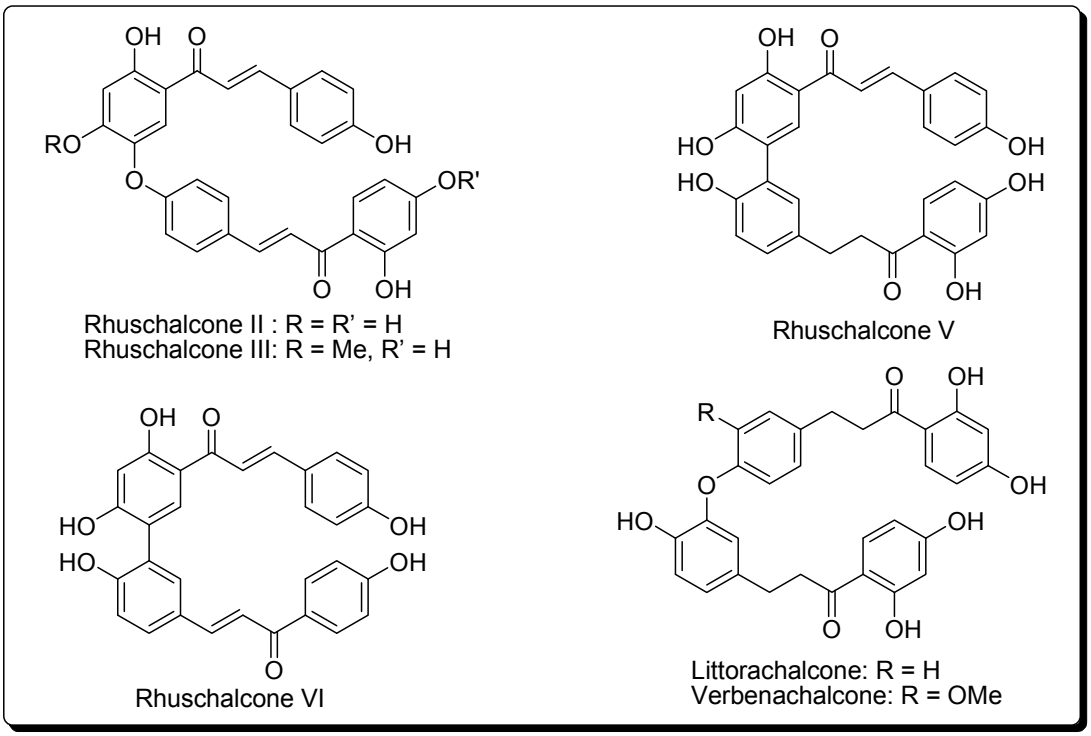

Figure 2. Untested bichalcones from *Rhus* species.

In order to rationalize the interaction of the identified hits in our study, all docking poses for sirt1 (PDB ID: 4ZZJ) and sirt2 (PDB ID: 4R8M and PDB ID: 5D7P) were analyzed using the MOE program [54]. Docking to sirt1 suggested two possible binding modes for the most active hits, compound **8** and **9** (Fig. 3a and S3). The most favourable (top score) binding mode was observed in the peptide binding pocket, where the hydroxyl group on the ring A of compound **9** interacts with

Preprints (www.preprints.org) | NOT PEER-REVIEWED | Posted: 23 January 2018 doi:10.20944/preprints201801.0213.v1

the backbone of the residue Gly415. A similar interaction was also observed for the co-crystallized peptide substrate [45]. Moreover, the hydroxyl groups on the ring A' of two active compounds were making additional H-bonds with the backbone carbonyl group of Gln345 residue. Although compound **8** does not show H-bonding with Asp348, we assume both compounds have the same binding mode, as the experimentally measured inhibitory potencies are very close in all measured sirtuin isoforms. Moreover, an H-bond interaction was formed between the hydroxyl group of ring B' of compound **9** and the side chain of the residue Asp348. With regards to binding to the sirt2 peptide pocket, H-bonds were observed between the hydroxyl groups in ring A of the actives and the O atom of Val233 in the protein backbone (Fig. 3b).

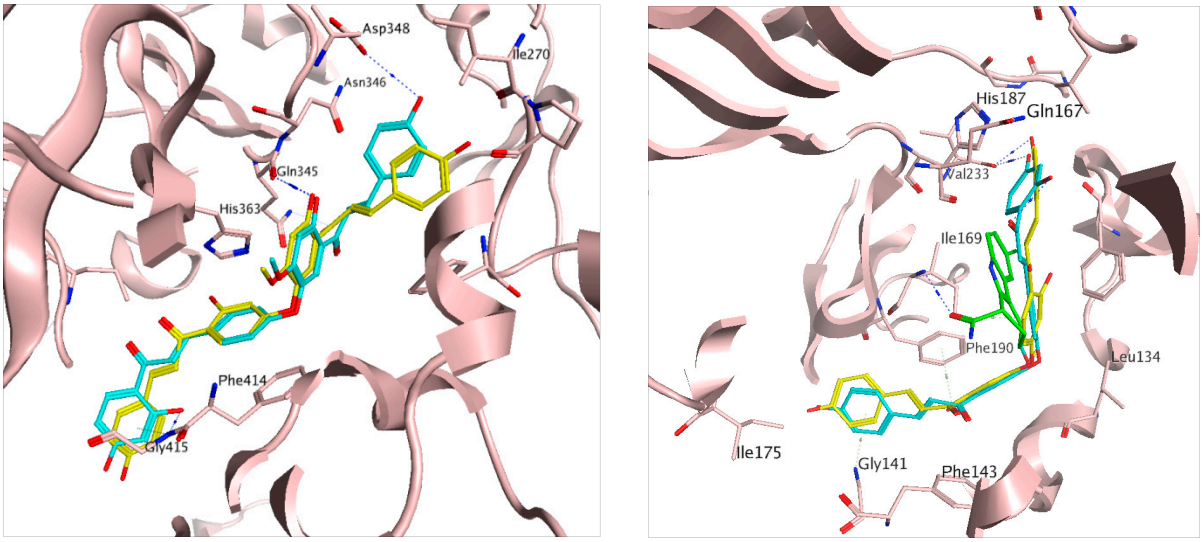

(**a**) (**b**)

Figure 3. Predicted common binding mode of active compounds in the peptide binding pockets of (**a**) sirt1(PDB ID: 4ZZJ) and (**b**) sirt2 (PDB ID: 4R8M). In both cases, compound 8 in yellow, compound 9 in cyan, hydrogen bonds drawn as dashed lines, while EX-243 is shown in green on subfigure (**b**).

The same interactions were observed for the myristol peptide as well in the X-ray structure of Sirt2, but not the same interactions as with the indole derivative EX-243 (Fig. 3b). Within the sirt2 extended C pocket (Fig. S4), the hydroxyl groups of the B' ring of the actives interact with His187 *via* the co-crystallized water molecule HOH676. Meanwhile, the hydroxyl groups of ring A interact with the O atom of Asp 170 in the backbone and the carbonyl groups (near the ring A') interact with the side chain of IIe232 (Fig. S4). Binding in the peptide pockets of both sirt1 and sirt2 are more driven by hydrophobic interactions than by H-bonding, explaining the similar activities against both sirtuin isoforms.

4. Materials and Methods

4.1. Database preparation

Ligand preparation of the 463 natural compounds in the p-ANAPL database was carried out using the LigPrep module in Schrödinger [55]. 10 low energy conformers were generated for each molecule and MMFF94 force field [56] implemented in MOE [54][15] was used for minimization. Pan-Assay Interference (PAIN) filters were applied using Schrodinger's Canvas tool [57] and CbLigand web server [58].

Preprints (www.preprints.org) | NOT PEER-REVIEWED | Posted: 23 January 2018 doi:10.20944/preprints201801.0213.v1

4.2. Protein preparation

All protein X-ray structures were retrieved from the Protein Data Bank (PDB) [59]. Protein preparation of different crystal structures of human sirt1 (PDB IDs: 4I5I [44], and 4ZZJ [45]), was carried out as detailed in the Supplementary Material, while sirt2 protein structures were prepared as previously described [36] (details in Supplementary Material). The docking procedure was performed using GOLD program (The Cambridge Crystallographic Data Centre, CCDC, Cambridge, UK) [60-62], preceded by preparation of the ligands using the LigPrep (Schrödinger, LLC, New York, NY, 2014) [55] tool in Maestro (Schrödinger, LLC, New York, NY, 2014) [61]. Hydrogen atoms were added to the ligand molecules, followed by minimization, using MMFFs force field in Maestro [63]. The crystal structure in complex with NAD^+ (PDB ID: 4I5I), along with the crystal structure co-crystallized with the acetyl lysine peptide (PDB ID: 4ZZJ), were used in the study. The protein structures were protonated and minimized, using the Amber 99SB force field, implemented in MOE [54].

4.3. Docking, scoring and hit selection

All water molecules, the cofactor and the peptide were removed. The location of the native ligand (NAD^+ or peptide) was used to define the docking site, where all protein residues within 6 Å from any heavy atom of this ligand were considered as part of the binding site. GoldScore was used as the fitness function to score all docking poses. All docking poses were analyzed by visual inspection and some compounds were chosen to be tested by *in vitro* assays, following a protocol to be given later. In the next step, ligands were docked into the substrate-binding pocket of human sirt1 and sirt2. This was carried out using two different docking programs (Gold [60-62] and Maestro [63]). The resulting docking poses were stored. The selection of compounds for testing was carried out by examining protein-ligand interactions in the derived docking poses. In the crystal structures of sirt1, it was shown that substrates make H-bond interactions with the backbone of a conserved valine residue (sirt1 numbering Val412) which is crucial for the correct orientation of the acyl-lysine in the active site [44]. In case of sirt2, we first examined the binding interactions of the native ligands including both the peptide substrates, the cofactor fragments and the co-crystallized inhibitors with the protein [31-43]. In the hit selection process, a special importance was given to compounds that were able to interact with residues Phe234, Phe235, Phe190 and Glu237 in the catalytic pocket. Seven compounds (**1**, **2**, **8**-**10**, **12** and **13**, Fig. 1) were identified as hits and retained for testing. All molecules, except the zinc ion (Zn^{2+}), were removed from the structures prior to docking. Structural bridging water molecules (where mentioned), were included in the binding site of the protein structures before docking. Docking studies were performed using the Glide program (Schrödinger Suite 2012-5.8) [64, 65]. The dockings were done using Glide high-throughput virtual screening (HTVS) mode, treating ligands flexibly. 10 docking poses were calculated for each conformer. Only the top-ranked poses were retained for each compound for each docking run. Docking poses retrieved for the top-ranked 20 compounds (~5% of the whole database) were visually analyzed, the hits being retained based on observed protein-ligand interactions within the target site. In sorting ligand poses by observed protein-ligand interactions, the emphasis was laid on ligand poses with putative interactions within the cofactor (NAD^+) and peptide binding pockets.

 doi:10.20944/preprints201801.0213.v1

4.4. In vitro assay

Human sirt1$_{133-747}$ was expressed as a GST-tagged enzyme and purified as described previously [66]. Human sirt2$_{56-356}$ and sirt3$_{118-395}$ were expressed as an N-terminally His$_6$-tagged enzyme and purified as described previously. The identity and purity of the produced enzymes were verified using SDS-PAGE [67]. Protein concentration was determined by the Bradford assay [68]. Deacetylase activity of sirtuin isoforms was NAD^+-dependent and could be inhibited by nicotinamide. Compound samples were provided from the p-ANAPL compound collection in Botswana, which has been stored below 0°C. The inhibitory activity against hSirt1, hSirt2 and hSirt3 was determined by a histone deacetylase assay, previously established [69], with further details provided in the Supplementary Material. Human sirt1$_{133-747}$, sirt2$_{25-389}$ or human sirt3$_{118-395}$ were mixed with assay buffer (50 mM Tris, 137 mM NaCl, 2.7 mM KCl, pH 8.0), NAD^+ (final assay concentration 500 µM), the substrate Z-(Ac)Lys-AMC, also termed ZMAL (final assay concentration 10,5 µM), the inhibitor dissolved in DMSO at various concentrations or DMSO as a control (final DMSO concentration 5% (v/v)). Total substrate conversion of controls was driven to about 15% - 30% to assure initial state conditions. The assay was carried out in 96-well plates with a reaction volume of 60 µL per well. All determinations were performed in triplicates. After an incubation for 4 h at 37 °C and 140 rpm, deacetylation was stopped by addition of 60 µL of a solution containing trypsin and nicotinamide (50 mMTris, 100 mMNaCl, 6.7% (v/v) DMSO, trypsin 16.5 U/µL, 8 mM nicotinamide, pH 8.0). The microplate was further incubated for 20 min at 37 °C and 140 rpm. Finally, fluorescence intensity was measured in a microplate reader (BMG Polarstar, λ_{ex} 390nm, λ_{em} 460nm). All compounds were pretested on auto-fluorescence, amino-methylcoumarin (AMC) quenching, and trypsin inhibition under assay conditions. Rates of inhibition were calculated by using the controls, containing no inhibitor, as a reference. GraphPad Prism software (La Jolla, USA) was employed to determine IC_{50} values.

5. Conclusions

In the present work, we combined target-based virtual screening with experimental testing in order to identify novel modulators of sirt1 and sirt2 within the p-ANAPL database. Molecular docking studies onto available sirt1 and sirt2 crystal structures resulted in two sirt1 and sirt2 inhibitors with moderate inhibitory effect. Although the rhuschalcones **8** and **9** have been known to possess other biological activities [47-52], it is yet unclear if their cytotoxicities are related to their abilities to inhibit sirtuins. However, natural product libraries like the p-ANAPL and the newly developed NANPDB [70] libraries could be good sources to search for novel modulators of sirtuins with novel scaffolds.

Supplementary Materials: The following are available online at www.mdpi.com/link, Figure S1. 13 selected compounds on the hit list: black (> 1 mg), red (tested negative) greed (active); Figure S2. Complete workflow of the *in silico* and *in vitro* screening processes; Figure S3. Predicted common binding mode of active compounds in the peptide binding pockets of Sirt2 (PDB ID: 4R8M): compound 8 in yellow, compound 9 in cyan, hydrogen bonds drawn as dashed lines); Figure S4. Predicted common binding mode of active compounds in the extended C pocket of Sirt2 (left: PDB ID: 5D7P) and the pocket surface is colored according to hydrophobic (green) and hydrophilic (pink) regions Sirt2 (right). Compound 8 in yellow, compound 9 in cyan, hydrogen bonds drawn as dashed lines); Figure S5. Predicted common binding mode of active compounds in the peptide binding pocket of sirt1 (PDB ID: 4ZZJ), with compound 8 shown in yellow, compound 9 in cyan, hydrogen bonds are drawn as dashed lines and EX-243 in green; Protein Preparation Protocols and detailed *in vitro* assay description.

Acknowledgments: ZA is currently a doctoral candidate financed by the German Academic Exchange Services (DAAD), Germany. FNK acknowledges a Georg Forster fellowship from the Alexander von Humboldt Foundation, Germany. The Jung group owes thanks to the German Research Foundation (DFG, within GRK1976) for support.

Author Contributions: F.N.K., W.S., K.A.M. and M.J. conceived and designed the experiments; B.K., Z.A., S.S., S.O.M. and F.N.K performed the experiments; B.K., Z.A., S.S., S.O.M. and F.N.K analyzed the data; W.S. S.O.M, K.A.M. and M.J. contributed reagents/materials/analysis tools; B.K. Z.A. and F.N.K. wrote the paper. All authors approved the final submission.

Conflicts of Interest: The authors declare no conflict of interest.

References

1. Harvey, A. L.; Edrada-Ebel, R.; Quinn, R. J. The re-emergence of natural products for drug discovery in the genomics era. *Nat Rev Drug Discov*. **2015**, *14*, 111-129. DOI: 10.1038/nrd4510.
2. Rodrigues, T.; Reker, D.; Schneider, P.; Schneider, G. Counting on natural products for drug design. *Nat Chem*. **2016**, *8*, 531-541. DOI: 10.1038/nchem.2479.
3. Mishra, B. B.; Tiwari, V. K. Natural products: an evolving role in future drug discovery. *Eur J Med Chem*. **2011**, *46*, 4769-4807. DOI: 10.1016/j.ejmech.2011.07.057.
4. Harvey, A. L. Natural products as a screening resource. *Curr Opin Chem Biol*. **2007**, *11*, 480-484. DOI: 10.1016/j.cbpa.2007.08.012
5. Newman, D. J.; Cragg, G. M. Natural products as sources of new drugs from 1981 to 2014. *J Nat Prod*. **2016**, *79*, 629-661. DOI: 10.1021/acs.jnatprod.5b01055.
6. Ntie-Kang, F.; Nwodo, J. N.; Ibezim, A.; Simoben, C. V.; Karaman, B.; Ngwa, V. F.; Sippl, W.; Adikwu, M. U.; Mbaze, L. M. Molecular modeling of potential anticancer agents from African medicinal plants. *J Chem Inf Model*. **2014**, *54*, 2433-2450. DOI: 10.1021/ci5003697.
7. Ntie-Kang, F.; Simoben, C. V.; Karaman, B.; Ngwa, V. F.; Judson, P. N.; Sippl, W.; Mbaze, L. M. Pharmacophore modeling and *in silico* toxicity assessment of potential anticancer agents from African medicinal plants. *Drug Des Devel Ther*. **2016**, *10*, 2137-2154. DOI: 10.2147/DDDT.S108118.
8. Ntie-Kang, F.; Zofou, D.; Babiaka, S. B.; Meudom, R.; Scharfe, M.; Lifongo, L. L.; Mbah, J. A.; Mbaze, L. M.; Sippl, W.; Efange, S. M. N. AfroDb: a select highly potent and diverse natural product library from African medicinal plants. *PLoS One*. **2013**, *8*, e78085. DOI: 10.1371/journal.pone.0078085.
9. Zofou, D.; Ntie-Kang, F.; Sippl, W.; Efange, S. M. N. Bioactive natural products derived from the Central African flora against neglected tropical diseases and HIV. *Nat Prod Rep*. **2013**, *30*, 1098-1120. DOI: 10.1039/c3np70030e.
10. Ntie-Kang, F.; Onguéné, P. A.; Fotso, G. W.; Andrae-Marobela, K.; Bezabih, M.; Ndom, J. C.; Ngadjui, B. T.; Ogundaini, A. O.; Abegaz, B. M.; Meva'a, L. M. Virtualizing the p-ANAPL library: a step towards drug discovery from African medicinal plants. *PLoS One*. **2014**, *9*, e90655. DOI: 10.1371/journal.pone.0090655.
11. Tietjen, I.; Ntie-Kang, F.; Mwimanzi, P.; Onguéné, P. A.; Scull, M. A.; Idowu, T. O.; Ogundaini, A. O.; Meva'a, LM.; Abegaz, B. M.; Rice, C. M.; Andrae-Marobela, K.; Brockman, M. A.; Brumme, Z. L.; Fedida, D. Screening of the pan-African natural product library identifies ixoratannin A-2 and boldine as novel HIV-1 inhibitors. *PLoS One*. **2015**, *10*, e0121099. DOI: 10.1371/journal.pone.0121099.
12. Park, J. B. Finding potent sirt inhibitor in coffee: isolation, confirmation and synthesis of javamide-II (*N*-caffeoyltryptophan) as sirt1/2 inhibitor. *PLoS One*. **2016**, *11*, e0150392. DOI: 10.1371/journal.pone.0150392.
13. Kokkonen, P.; Kokkola, T.; Suuronen, T.; Poso, A.; Jarho, E.; Lahtela-Kakkonen, M. Virtual screening approach of sirtuin inhibitors results in two new scaffolds. *Eur J Pharm Sci*. **2015**, *76*, 27-32. DOI: 10.1016/j.ejps.2015.04.025.
14. Salo, H. S.; Laitinen, T.; Poso, A.; Jarho, E.; Lahtela-Kakkonen, M. Identification of novel Sirt3 inhibitor scaffolds by virtual screening. *Bioorg Med Chem Lett*. **2013**, *23*, 2990-2995. DOI: 10.1016/j.bmcl.2013.03.033.
15. Sacconnay, L.; Angleviel, M.; Randazzo, G. M.; Queiroz, M. M.; Queiroz, E. F.; Wolfender, J. L.; Carrupt, P. A.; Nurisso, A. Computational studies on sirtuins from *Trypanosoma cruzi*: structures, conformations and interactions with phytochemicals. *PLoS Negl Trop Dis*. **2014**, *8*, e2689. DOI: 10.1371/journal.pntd.0002689.
16. Sun, Y.; Zhou, H.; Zhu, H.; Leung, S. W. Ligand-based virtual screening and inductive learning for identification of Sirt1 inhibitors in natural products. *Sci Rep*. **2016**, *6*, 19312. DOI: 10.1038/srep19312.

17. Sacconnay, L.; Ryckewaert, L.; Randazzo, G. M.; Petit, C.; Passos Cdos, S.; Jachno, J.; Michailovienė, V.; Zubrienė, A.; Matulis, D.; Carrupt, PA.; Simões-Pires, C. A.; Nurisso, A. 5-Benzylidene-hydantoin is a new scaffold for Sirt inhibition: From virtual screening to activity assays. *Eur J Pharm Sci*. **2016**, *85*, 59-67. DOI: 10.1016/j.ejps.2016.01.010.
18. Liu, S.; Ji, S.; Yu, Z. Y.; Wang, H. L.; Cheng, X.; Li, W. J.; Jing, L.; Yu, Y.; Chen, Q.; Yang, L. L.; Li, G. B.; Wu, Y. Structure-based discovery of new selective small-molecule sirtuin 5 inhibitors. *Chem Biol Drug Des*. **2017**, *91*, 257-268. DOI: 10.1111/cbdd.13077.
19. Padmanabhan, B.; Ramu, M.; Mathur, S.; Unni, S.; Thiyagarajan, S. Identification of new inhibitors for human sirt1: an *in-silico* approach. *Med Chem*. **2016**, *12*, 347-361. DOI: 10.2174/1573406412666160107111612
20. Pulla, V. K.; Sriram, D. S.; Viswanadha, S.; Sriram, D.; Yogeeswari, P. Energy-based pharmacophore and three-dimensional quantitative structure-activity relationship (3D-QSAR) modeling combined with virtual screening to identify novel small-molecule inhibitors of silent mating-type information regulation 2 homologue 1 (sirt1). *J Chem Inf Model*. **2016**, *56*, 173-187. DOI: 10.1021/acs.jcim.5b00220.
21. Haigis, M. C.; Sinclair, D. A. Mammalian sirtuins: biological insights and disease relevance. *Annu Rev Pathol*. **2010**, *5*, 253-295. DOI: 10.1146/annurev.pathol.4.110807.092250.
22. Howitz, K. T.; Bitterman, K. J.; Cohen, H. Y.; Lamming, D. W.; Lavu, S.; Wood, J. G.; Zipkin, R. E.; Chung, P.; Kisielewski, A.; Zhang, L. L.; Scherer, B.; Sinclair, D. A. Small molecule activators of sirtuins extend *Saccharomyces cerevisiae* lifespan. *Nature*. **2003**, *425*, 191-196. DOI: 10.1038/nature01960
23. Feige, J. N.; Lagouge, M.; Canto, C.; Strehle, A.; Houten, S. M.; Milne, J. C.; Lambert, P. D.; Mataki, C.; Elliott, P. J.; Auwerx, J. Specific Sirt1 activation mimics low energy levels and protects against diet-induced metabolic disorders by enhancing fat oxidation. *Cell Metab*. **2008**, *8*, 347-358. DOI: 10.1016/j.cmet.2008.08.017.
24. Gallí, M.; van Gool, F.; Leo, O. Sirtuins and inflammation: friends or foes? *Biochem Pharmacol*. **2011**, *81*, 569-576. DOI: 10.1016/j.bcp.2010.12.010.
25. Vachharajani, V. T.; Liu, T.; Wang, X.; Hoth, J. J.; Yoza, B. K.; McCall, C. E. Sirtuins link inflammation and metabolism. *J Immunol Res*. **2016**, *2016*, 8167273. DOI: 10.1155/2016/8167273.
26. Outeiro, T. F.; Kontopoulos, E.; Altmann, S. M.; Kufareva, I.; Strathearn, K. E.; Amore, A. M.; Volk, C. B.; Maxwell, M. M.; Rochet, J. C.; McLean, P. J.; Young, A. B.; Abagyan, R.; Feany, M. B.; Hyman, B. T.; Kazantsev, A. G. Sirtuin 2 inhibitors rescue alpha-synuclein-mediated toxicity in models of Parkinson's disease. *Science*. **2007**, *317*, 516-519. DOI: 10.1126/science.1143780
27. Luthi-Carter, R.; Taylor, D. M.; Pallos, J.; Lambert, E.; Amore, A.; Parker, A.; Moffitt, H.; Smith, D. L.; Runne, H.; Gokce, O.; Kuhn, A.; Xiang, Z.; Maxwell, M. M.; Reeves, S. A.; Bates, G. P.; Neri, C.; Thompson, L. M.; Marsh, J. L.; Kazantsev, A. G. Sirt2 inhibition achieves neuroprotection by decreasing sterol biosynthesis. *Proc Natl Acad Sci USA*. **2010**, *107*, 7927-7932. DOI: 10.1073/pnas.1002924107.
28. Hu, J.; Jing, H.; Lin, H. Sirtuin inhibitors as anticancer agents. *Future Med Chem*. **2014**, *6*, 945-966. DOI: 10.4155/fmc.14.44.
29. Li, X. Sirt1 and energy metabolism. *Acta Biochim Biophys Sin (Shanghai)*. **2013**, *45*, 51-60. DOI: 10.1093/abbs/gms108.
30. Davenport, A. M.; Huber, F. M.; Hoelz, A. Structural and functional analysis of human Sirt1. *J Mol Biol*. **2014**, *426*, 526-541. DOI: 10.1016/j.jmb.2013.10.009.
31. Jin, J.; He, B.; Zhang, X.; Lin, H.; Wang, Y. Sirt2 reverses 4-oxononanoyl lysine modification on histones. *J Am Chem Soc*. **2016**, *138*, 12304-12307. DOI: 10.1021/jacs.6b04977.
32. Moniot, S.; Forgione, M.; Lucidi, A.; Hailu, G. S.; Nebbioso, A.; Carafa, V.; Baratta, F.; Altucci, L.; Giacché, N.; Passeri, D.; Pellicciari, R.; Mai, A.; Steegborn, C.; Rotili, D. Development of 1,2,4-oxadiazoles as potent and selective inhibitors of the human deacetylase sirtuin 2: structure-activity relationship, X-ray crystal structure, and anticancer activity. *J Med Chem*. **2017**, *60*, 2344-2360. DOI: 10.1021/acs.jmedchem.6b01609.
33. Sundriyal, S.; Moniot, S.; Mahmud, Z.; Yao, S.; Di Fruscia, P.; Reynolds, C. R.; Dexter, D. T.; Sternberg, M. J.; Lam, E. W.; Steegborn, C.; Fuchter, M. J. Thienopyrimidinone based sirtuin-2 (sirt2)-selective inhibitors bind in the ligand induced selectivity pocket. *J Med Chem*. **2017**, *60*, 1928-1945. DOI: 10.1021/acs.jmedchem.6b01690.
34. Knyphausen, P.; de Boor, S.; Kuhlmann, N.; Scislowski, L.; Extra, A.; Baldus, L.; Schacherl, M.; Baumann, U.; Neundorf, I.; Lammers, M. Insights into lysine deacetylation of natively folded substrate proteins by sirtuins. *J Biol Chem*. **2016**, *291*, 14677-14694. DOI: 10.1074/jbc.M116.726307.

35. Schiedel, M.; Rumpf, T.; Karaman, B.; Lehotzky, A.; Gerhardt, S.; Ovádi, J.; Sippl, W.; Einsle, O.; Jung, M. Structure-based development of an affinity probe for sirtuin 2. *Angew Chem Int Ed Engl*. **2016**, *55*, 2252-2256. DOI: 10.1002/anie.201509843.
36. Schiedel, M.; Rumpf, T.; Karaman, B.; Lehotzky, A.; Oláh, J.; Gerhardt, S.; Ovádi, J.; Sippl, W.; Einsle, O.; Jung, M. Aminothiazoles as potent and selective sirt2 inhibitors: a structure-activity relationship study. *J Med Chem*. **2016**, *59*, 1599-1612. DOI: 10.1021/acs.jmedchem.5b01517.
37. Feldman, J. L.; Dittenhafer-Reed, K. E.; Kudo, N.; Thelen, J. N.; Ito, A.; Yoshida, M.; Denu, J. M. Kinetic and structural basis for acyl-group selectivity and NAD(+) dependence in sirtuin-catalyzed deacylation. *Biochemistry*. **2015**, *54*, 3037-3050. DOI: 10.1021/acs.biochem.5b00150.
38. Rumpf, T.; Gerhardt, S.; Einsle, O.; Jung, M. Seeding for sirtuins: microseed matrix seeding to obtain crystals of human Sirt3 and Sirt2 suitable for soaking. *Acta Crystallogr F Struct Biol Commun*. **2015**, *71*, 1498-1510. DOI: 10.1107/S2053230X15019986.
39. Teng, Y. B.; Jing, H.; Aramsangtienchai, P.; He, B.; Khan, S.; Hu, J.; Lin, H.; Hao, Q. Efficient demyristoylase activity of Sirt2 revealed by kinetic and structural studies. *Sci Rep*. **2015**, *5*, 8529. DOI: 10.1038/srep08529.
40. Rumpf, T.; Schiedel, M.; Karaman, B.; Roessler, C.; North, B. J.; Lehotzky, A.; Oláh, J.; Ladwein, K. I.; Schmidtkunz, K.; Gajer, M.; Pannek, M.; Steegborn, C.; Sinclair, D. A.; Gerhardt, S.; Ovádi, J.; Schutkowski, M.; Sippl, W.; Einsle, O.; Jung, M. Selective Sirt2 inhibition by ligand-induced rearrangement of the active site. *Nat Commun*. **2015**, *6*, 6263. DOI: 10.1038/ncomms7263.
41. Yamagata, K.; Goto, Y.; Nishimasu, H.; Morimoto, J.; Ishitani, R.; Dohmae, N.; Takeda, N.; Nagai, R.; Komuro, I.; Suga, H.; Nureki, O. Structural basis for potent inhibition of Sirt2 deacetylase by a macrocyclic peptide inducing dynamic structural change. *Structure*. **2014**, *22*, 345-352. DOI: 10.1016/j.str.2013.12.001.
42. Moniot, S.; Schutkowski, M.; Steegborn, C. Crystal structure analysis of human Sirt2 and its ADP-ribose complex. *J Struct Biol*. **2013**, *182*, 136-43. DOI: 10.1016/j.jsb.2013.02.012.
43. Finnin, M. S.; Donigian, J. R.; Pavletich, N. P. Structure of the histone deacetylase Sirt2. *Nat Struct Biol*. **2001**, *8*, 621-625. DOI: 10.1038/89668
44. Zhao, X.; Allison, D.; Condon, B.; Zhang, F.; Gheyi, T.; Zhang, A.; Ashok, S.; Russell, M.; MacEwan, I.; Qian, Y.; Jamison, J. A.; Luz, J. G. The 2.5 Å crystal structure of the Sirt1 catalytic domain bound to nicotinamide adenine dinucleotide (NAD^+) and an indole (EX527 analogue) reveals a novel mechanism of histone deacetylase inhibition. *J Med Chem*. **2013**, *56*, 963-969. DOI: 10.1021/jm301431y.
45. Dai, H.; Case, A. W.; Riera, T. V.; Considine, T.; Lee, J. E.; Hamuro, Y.; Zhao, H.; Jiang, Y.; Sweitzer, S. M.; Pietrak, B.; Schwartz, B.; Blum, C. A.; Disch, J. S.; Caldwell, R.; Szczepankiewicz, B.; Oalmann, C.; Yee Ng, P.; White, B. H.; Casaubon, R.; Narayan, R.; Koppetsch, K.; Bourbonais, F.; Wu, B.; Wang, J.; Qian, D.; Jiang, F.; Mao, C.; Wang, M.; Hu, E.; Wu, J. C.; Perni, R. B.; Vlasuk, G. P.; Ellis, J. L. Crystallographic structure of a small molecule Sirt1 activator-enzyme complex. *Nat Commun*. **2015**, *6*, 7645. DOI: 10.1038/ncomms8645.
46. Masesane, I. B.; Yeboah, S. O.; Liebscher, J.; Mügge, C.; Abegaz, B. M. A bichalcone from the twigs of *Rhus pyroides*. *Phytochemistry*. **2000**, *53*, 1005-1008. DOI: 10.1016/S0031-9422(99)00553-1
47. Mdee, L. K.; Yeboah, S. O.; Abegaz, B. M. Rhuschalcones II-VI, five new bichalcones from the root bark of *Rhus pyroides*. *J Nat Prod*. **2003**, *66*, 599-604. DOI: 10.1021/np020138q
48. Shetonde, O.; Mdee, L.; Bezibih, M.; Mammo, W.; Abegaz, B. The characterization, total synthesis and antiprotozoal activities of novel bichalcones from *Rhus pyroides*. *Planta Med*. **2009**, *75*, SL11. DOI: 10.1055/s-0029-1234266
49. Mihigo, S. O.; Mammo, W.; Bezabih, M.; Andrae-Marobela, K.; Abegaz, B. M. Total synthesis, antiprotozoal and cytotoxicity activities of rhuschalcone VI and analogs. *Bioorg Med Chem*. **2010**, *18*, 2464-2473. DOI: 10.1016/j.bmc.2010.02.055.
50. Arslan, T.; Çelik, G.; Çelik, H.; Sentürk, M.; Yayli, N.; Ekinci, D. Synthesis and biological evaluation of novel bischalcone derivatives as carbonic anhydrase inhibitors. *Arch Pharm Chem Life Sci*. **2016**, *349*, 741-748. DOI: 10.1002/ardp.201600122.
51. Svenningsen, A. B.; Madsen, K. D.; Liljefors, T.; Stafford, G. I.; van Staden, J.; Jäger, A. K. Biflavones from *Rhus* species with affinity for the $GABA_A$/benzodiazepine receptor. *J Ethnopharmacol*. **2006**, *103*, 276-280. DOI: 10.1016/j.jep.2005.08.012
52. Zhang, Y.; Chen, Y.; Yang, Y.; Guan X. The synthesis of bichalcone rhuschalcone I. *Chinese J Appl Chem*. **2011**, *28*, 652-656.

53. Kahyo, T.; Ichikawa, S.; Hatanaka, T.; Yamada, M. K.; Setou, M. A novel chalcone polyphenol inhibits the deacetylase activity of Sirt1 and cell growth in HEK293T cells. *J Pharmacol Sci*. **2008**, *108*, 364-371. DOI: 10.1254/jphs.08203FP
54. Molecular Operating Environment, Chemical Computing Group Inc., Montreal, **2014**.
55. LigPrep Software, Version 2.5; LLC: New York, **2011**.
56. Halgren, T. A. Merck molecular forcefield. *J Comput Chem*. **1996**, *17*, 490-641. DOI: 10.1002/(SICI)1096-987X
57. Canvas, Schrödinger, LLC, New York, **2017**.
58. Baell, J. B.; Holloway, G. A. New substructure filters for removal of Pan Assay Interference Compounds (PAINS) from screening libraries and for their exclusion in bioassays. *J Med Chem*. **2010**, *53*, 2719-2740. DOI: 10.1021/jm901137j, (http://cbligand.org/PAINS/). Last Assessed 20 January 2018
59. Berman, H. M.; Westbrook, J.; Feng, Z.; Gilliland, G.; Bhat, T. N.; Weissig, H.; Shindyalov, I. N.; Bourne, P. E. The Protein Data Bank. *Nucleic Acids Res*. **2000**, *28*, 235-42. PMID: 10592235.
60. Jones, G.; Willett, P.; Glen, R. C.; Leach, A. R.; Taylor, R. Development and validation of a genetic algorithm for flexible docking. *J Mol Biol*. **1997**, *267*, 727-748. DOI: 10.1006/jmbi.1996.0897
61. Jones, G.; Willett, P.; Glen, R. C. Molecular recognition of receptor sites using a genetic algorithm with a description of desolvation. *J Mol Biol*. **1995**, *245*, 43-53. DOI: 10.1016/S0022-2836(95)80037-9
62. Verdonk, M. L.; Cole, J. C.; Hartshorn, M. J.; Murray, C. W.; Taylor, R. D. Improved protein-ligand docking using GOLD. *Proteins*. **2003**, *52*, 609-623. DOI: 10.1002/prot.10465
63. Maestro (Schrödinger, LLC, New York, NY, 2014), Maestro, Version 9.2; LLC: New York, **2011**;
64. Glide program (Schrödinger Suite 2012-5.8)
65. Friesner, R. A.; Banks, J. L.; Murphy, R. B.; Halgren, T. A.; Klicic, J. J.; Mainz, D. T.; Repasky, M. P.; Knoll, E. H.; Shelley, M.; Perry, J. K.; Shaw, D. E.; Francis, P.; Shenkin, P. S. Glide: a new approach for rapid, accurate docking and scoring. 1. Method and assessment of docking accuracy. *J Med Chem*. **2004**, *47*, 1739-1749. DOI: 10.1021/jm0306430
66. Schiedel, M.; Herp, D.; Hammelmann, S.; Swyter, S.; Lehotzky, A.; Robaa, D.; Oláh, J.; Ovádi, J.; Sippl, W.; Jung, M. Chemically induced degradation of sirtuin 2 (sirt2) by a proteolysis targeting chimera (PROTAC) based on sirtuin rearranging ligands (SirReals). *J Med Chem*. **2017**, DOI: 10.1021/acs.jmedchem.6b01872.
67. Laemmli, U. K. Cleavage of structural proteins during the assembly of the head of bacteriophage T4. *Nature*. **1970**, *227*, 680-685. PMID: 5432063
68. Bradford, M. M. A rapid and sensitive method for the quantitation of microgram quantities of protein utilizing the principle of protein-dye binding. *Anal Biochem*. **1976**, *72*, 248-254. DOI:10.1016/0003-2697(76)90527-3
69. Heltweg, B.; Trapp, J.; Jung, M. *In vitro* assays for the determination of histone deacetylase activity. *Methods*. **2005**, *36*, 332-337. DOI: 10.1016/j.ymeth.2005.03.003
70. Ntie-Kang, F.; Telukunta, KK.; Döring, K.; Simoben, C. V.; Moumbock, A. F.; Malange, Y. I.; Njume, L. E.; Yong, J. N.; Sippl, W.; Günther, S. NANPDB: a resource for natural products from Northern African sources. *J Nat Prod*. **2017**, *80*, 2067-2076. DOI: 10.1021/acs.jnatprod.7b00283.

Sample Availability: Samples of the compounds **8** and **9** are available from the authors.